

## Influence of autoionizing states on the pulse-length dependence of strong-field Ne<sup>+</sup> photoionization at 38.4 eV

Hamonou, L., Lysaght, M., & Van Der Hart, H. (2010). Influence of autoionizing states on the pulse-length dependence of strong-field Ne<sup>+</sup> photoionization at 38.4 eV. *Journal of Physics B: Atomic Molecular and Optical Physics*, 43(4), 045601. [045601]. DOI: 10.1088/0953-4075/43/4/045601

**Published in:**

Journal of Physics B: Atomic Molecular and Optical Physics

**Document Version:**

Peer reviewed version

**Queen's University Belfast - Research Portal:**

[Link to publication record in Queen's University Belfast Research Portal](#)

**General rights**

Copyright for the publications made accessible via the Queen's University Belfast Research Portal is retained by the author(s) and / or other copyright owners and it is a condition of accessing these publications that users recognise and abide by the legal requirements associated with these rights.

**Take down policy**

The Research Portal is Queen's institutional repository that provides access to Queen's research output. Every effort has been made to ensure that content in the Research Portal does not infringe any person's rights, or applicable UK laws. If you discover content in the Research Portal that you believe breaches copyright or violates any law, please contact [openaccess@qub.ac.uk](mailto:openaccess@qub.ac.uk).

## LETTER TO THE EDITOR

# Influence of autoionizing states on the pulse-length dependence of strong-field $\text{Ne}^+$ photoionization at 38.4 eV

Linda Hamonou, Michael A. Lysaght and Hugo W. van der Hart

Centre for Theoretical Atomic, Molecular and Optical Physics, Queen's University Belfast, Belfast BT7 1NN, United Kingdom

**Abstract.** Using the time-dependent R-matrix approach, we investigate ionization of ground-state  $\text{Ne}^+$ , irradiated by laser light with a photon energy of 38.4 eV at intensities  $10^{13} \text{ W cm}^{-2}$ ,  $2 \times 10^{13} \text{ W cm}^{-2}$  and  $10^{14} \text{ W cm}^{-2}$  as a function of pulse length. Although the photon energy is below the threshold for single-photon ionization, we obtain a significant contribution from single-photon ionization to the ionization probability due to the finite duration of the pulse. The two-photon ionization rates deduced from the calculations are consistent with those obtained in R-matrix-Floquet rate calculations. The ionization probability oscillates with pulse length, which is ascribed to population and depopulation of autoionizing states just above the  $\text{Ne}^{2+}$  ground state, reached after absorption of a single photon. At an intensity of  $10^{14} \text{ W cm}^{-2}$ , pulse lengths longer than 50 cycles are required for two-photon ionization to dominate the ionization probability.

PACS numbers: 32.80.Rm, 32.30.Rj

The development of free-electron lasers operating in the VUV and the X-ray domain has given experimentalists new ways of investigating multi-electron dynamics in strong laser fields. These new laser facilities have, for example, enabled experimentalists to investigate two-photon double ionization of Ne in the photon-energy regime where direct two-photon double ionization is energetically allowed, but sequential ( $\text{Ne} \rightarrow \text{Ne}^+ \rightarrow \text{Ne}^{2+}$ ) double ionization is energetically not allowed since the photon energy is not sufficient to ionize  $\text{Ne}^+$  with a single photon (eg. Sorokin *et al* 2007). At larger photon energies, sequential double ionization is allowed, but also in this process one can find signatures of the fact that the two different emission processes are not independent of each other (Fritzsche *et al* 2008).

One of the grand challenges in theoretical atomic physics is the description of multi-electron dynamics in complex atoms irradiated by intense laser pulses. Over the last 15 years, great progress has been made in the description of pure two-electron systems in intense laser fields, for example for two-photon double ionization processes (see, for example, Colgan *et al* 2002, Feng and van der Hart 2003, Laulan *et al* 2005, Feist *et al* 2008) as well as for multiphoton double ionization at 390 nm (Parker *et al* 2006). These calculations require substantial computational resources, such that the direct extension of these techniques to systems with more than two electrons, like Ne, is unfeasible at present. Other approaches are required to describe the behaviour of complex atoms in intense light fields.

The most successful approach for the description of complex atoms in intense laser light at present is the R-matrix-Floquet approach. This approach was designed from the outset to treat complex atoms in intense light fields by combining the R-matrix approach with the Floquet Ansatz (Burke *et al* 1991). It has been applied to a wide range of problems, ranging from strong-field ionization of Ne and Ar at 390 nm, requiring absorption of at least eight and six photons respectively, (van der Hart 2006) to two-photon emission of the inner 1s electron from ground-state  $\text{Li}^-$  (van der Hart 2005). More recently, the R-matrix-Floquet approach has been instrumental in indicating the importance of detailed atomic structure in two-photon ionization of  $\text{Ne}^+$  (Hamonou *et al* 2008, Hamonou and van der Hart 2008).

The theoretical investigation of ionization processes in  $\text{Ne}^+$  is of particular relevance at the moment, due to the large number of strong-field multiple ionization studies on Ne at photon energies in the range between 38 and 50 eV. Ionization yields of various Ne ions were obtained by Sorokin *et al* (2007) at photon energies below the  $\text{Ne}^+$  ionization threshold and above this threshold. Moshhammer *et al* (2007) obtained detailed recoil momentum spectra for two-photon double ionization of Ne at 44 eV. Rudenko *et al* (2008) found that these recoil-ion momentum distributions differed strongly from the recoil-ion momentum distributions for two-photon double ionization of He at 44 eV. At 44 eV, sequential double ionization is allowed for Ne, whereas it is not allowed for He. The dominance of sequential double ionization of Ne was demonstrated experimentally by Kurka *et al* (2009).

Whereas in previous work (Hamonou *et al* 2008, Hamonou and van der Hart 2009), we investigated the response of  $\text{Ne}^+$  ions to high-frequency laser light using the time-independent R-matrix-Floquet approach, elucidation of the dynamics in a complex atom requires an explicit time-dependent approach. The time-dependent investigation of  $\text{Ne}^+$  ionization is particularly relevant for a photon energy of 38.4 eV, chosen in experiment (Sorokin *et al* 2007). This photon energy lies 2.6 eV below the single-photon ionization threshold. For very short pulses the uncertainty principle will thus ensure that the bandwidth of the pulse extends beyond the threshold and single-photon ionization will thus be possible. However, even for longer pulses, single-photon ionization may still contribute significantly to the total ionization yield. Single-photon ionization can only occur in the edge of the bandwidth, but it requires absorption of only a single photon. Two-photon ionization is energetically allowed over the entire bandwidth of the pulse, but it requires absorption of an additional photon. Therefore, especially at lower intensities, one needs to account for the possibility of single-photon ionization occurring in the edge of the bandwidth.

The contribution of single-photon ionization in the edge of the bandwidth may be enhanced substantially in complex atoms, such as  $\text{Ne}^+$ . Its lowest ionization threshold is the  $\text{Ne}^{2+} 2s^2 2p^4 \ ^3P^e$  threshold. This is not an isolated threshold. Just a few eV above this threshold, the  $2s^2 2p^4 \ ^1D^e$  and  $\ ^1S^e$  states can be found.  $\text{Ne}^+$  Rydberg series are attached to each of these thresholds, and there are thus autoionizing states lying just above the  $\text{Ne}^{2+}$  threshold. These autoionizing states can have a substantial influence on the ionization yields, as demonstrated for example in photoionization experiments (Covington *et al* 2002). The influence of such autoionizing states can not be determined using the R-matrix-Floquet approach as this approach assumes a well-defined photon energy. Hence, we need to apply an approach capable of describing time-dependent dynamics as well as the atomic structure of complex atoms, and such a method is the time-dependent R-matrix approach.

At Queen's University Belfast, we have recently developed a time-dependent R-

matrix approach for the description of ultrafast multi-electron dynamics in complex atoms. Initially, we developed an approach in which the entire time-dependent problem was contained within an enlarged R-matrix inner region (van der Hart *et al* 2007). This approach was applied to strong-field photoionization of Ar, and excellent agreement between ionization rates obtained using the time-dependent approach and using the R-matrix-Floquet approach was observed. Subsequently, Lysaght *et al* (2008, 2009a) developed a time-dependent R-matrix approach which adheres to the R-matrix formalism: an inner region within which all electron-electron interactions are accounted for, and an outer region within which exchange and exchange-correlation interactions can safely be neglected. This latter approach was exploited to investigate dynamics following coherent excitation of states within a configuration enabling the investigation of multi-electron dynamics driven by electron-electron repulsion (Lysaght *et al* 2009b). A second time-dependent R-matrix approach, similar in nature to our initial approach, has been developed by Bartschat and co-workers (Guan *et al* 2008, 2009).

Ne<sup>+</sup> is described similar to our previous study of the contribution of inner-shell excitation and ionization processes to the two-photon ionization rates of Ne<sup>+</sup> (Hamonou and van der Hart 2008). Following ionization of Ne<sup>+</sup>, the residual Ne<sup>2+</sup> ion can be left in five states:  $2s^22p^4\ ^3P^e$ ,  $^1D^e$  and  $^1S^e$ , and  $2s2p^5\ ^3P^o$  and  $^1P^o$ . These states are generated using an orbital set containing 1s, 2s and 2p orbitals for the Hartree-Fock ground state of Ne<sup>+</sup> (Clementi and Roetti 1974), and 3s, 3p, 3d, 4s,  $\overline{4p}$  and  $\overline{4d}$  orbitals (McLaughlin and Bell 2000). From these orbitals we build a Ne<sup>2+</sup> basis set containing all single excitations of a 2s and 2p electron from  $1s^22s^22p^4$ ,  $1s^22s2p^5$  and  $1s^22p^6$ . A small configuration-interaction calculation then gives us the desired Ne<sup>2+</sup> target states. The Ne<sup>+</sup> basis is then generated by combining these target states with an extensive set of continuum orbitals. In addition, correlation orbitals are generated by combining the Ne<sup>2+</sup> CI basis functions with an additional function from the orbital set.

For the present time-dependent calculations, we include Ne<sup>+</sup> basis functions with total angular momentum up to  $L = 8$ . The box size used is 120 atomic units, and we use a continuum orbital set containing 150 functions. In order to prevent spurious reflections from the boundary, we include an absorbing boundary potential. We have also performed some calculations in larger box sizes, increasing the number of continuum orbitals and moving the absorbing boundary outward. No significant changes in the ionization yields were obtained. The characteristics of the chosen laser pulse are as follows. The photon energy is set to 38.4 eV. Calculations have been performed for three different intensities,  $10^{13}$  W cm<sup>-2</sup>,  $2 \times 10^{13}$  W cm<sup>-2</sup> and  $10^{14}$  W cm<sup>-2</sup>. The laser pulse has a three-cycle sin<sup>2</sup> turn-on of the amplitude of the electric field to its maximum value. The peak intensity is then maintained for a set number of cycles. Finally, the laser pulse is switched off using a three-cycle sin<sup>2</sup> turn-off of the amplitude of the electric field.

The main quantity of interest in the present application of the time-dependent R-matrix approach is the ionization probability. The ionization probabilities  $Y$  are obtained from the Ne<sup>+</sup> wavefunction at the end of the pulse as follows:

$$Y = 1 - \sum_{i, E_i < E_{\text{Ne}^{2+}(3P^e)}} |c_i|^2. \quad (1)$$

We thus calculate the population left in bound states of Ne<sup>+</sup> at the end of the pulse. The remainder of the initial population is considered ionization. Population left in

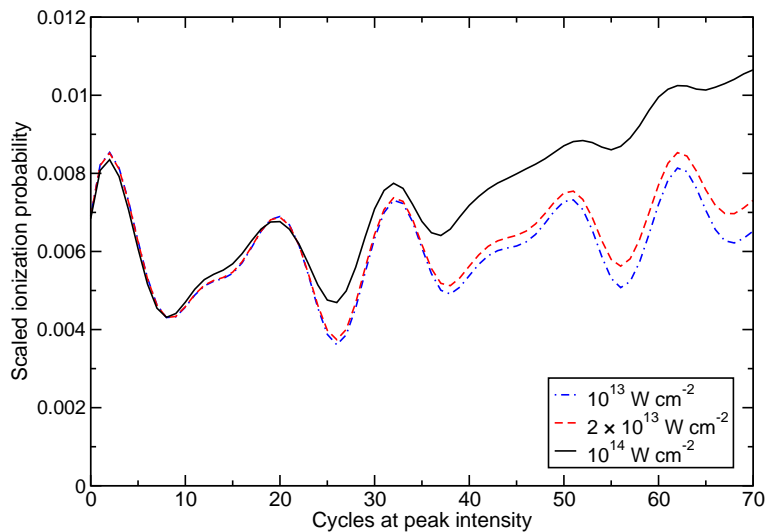


**Figure 1.** (Colour online) Scaled ionisation probabilities of  $\text{Ne}^+$  at a photon energy of 38.4 eV as a function of pulse length. The pulse consists of a three-cycle  $\sin^2$  turn-on, the given number of cycles at peak intensity and a three-cycle  $\sin^2$  turn-off. Yields are presented for three intensities:  $10^{13} \text{ W cm}^{-2}$  (blue dashed line),  $2 \times 10^{13} \text{ W cm}^{-2}$  (red dotted line with circles) and  $10^{14} \text{ W cm}^{-2}$  (black solid line). The ionization probability for  $10^{13} \text{ W cm}^{-2}$  is multiplied by a factor 10, and the ionization probability for  $2 \times 10^{13} \text{ W cm}^{-2}$  is multiplied by a factor 5.

bound states of  $\text{Ne}^+$  above the  $\text{Ne}^{2+}$  ground state is considered as ionization in the present approach. This is of course an approximation since such states may decay by photo-emission. We believe that the present approach nevertheless gives good insight into the physics of strong-field ionization of complex atoms by short VUV laser pulses.

Figure 1 shows the obtained  $\text{Ne}^+$  ionization probabilities as a function of pulse length for the three intensities considered in the present work,  $10^{13} \text{ W cm}^{-2}$ ,  $2 \times 10^{13} \text{ W cm}^{-2}$  and  $10^{14} \text{ W cm}^{-2}$ . To improve the comparison between the ionization probabilities, the ones obtained for an intensity of  $10^{13} \text{ W cm}^{-2}$  are multiplied by a factor 10, and the ones obtained for an intensity of  $2 \times 10^{13} \text{ W cm}^{-2}$  are multiplied by a factor 5. The probabilities are of similar magnitude for all pulse lengths even though the total pulse length varies over one order of magnitude: from 6 cycles (0 cycles at peak intensity) to 76 cycles (70 at peak intensity).

A closer inspection of figure 1 leads to the identification of three distinct features in the behaviour of the ionization probability with pulse length. A maximum in the ionization probability is obtained for a very short pulse length, and it takes substantially longer pulses for the ionization probability to reach a similar value subsequently. The differences between the scaled ionization probabilities with different intensities are very small for short pulses, and appear to increase only for pulses longer than about 15 cycles at peak intensity. The ionization probabilities show substantial oscillations with pulse length, with a total variation in the probability of the order of over 30-50% of the probability.

Since the background part of the total ionization probability shown in figure 1 scales linearly with intensity, figure 1 suggests that, for the current set of pulse

lengths and intensities, the dominant contribution to the ionization probability is given by ionization processes involving the absorption of a single photon. The first reason for this dominance is that in a time-dependent picture, the laser pulse has a turn-on and a turn-off. In the present study, these are given by a three-cycle  $\sin^2$  behaviour. In the frequency domain, the turn-on and turn-off give rise to additional frequency components. If these are sufficiently rapid, as is the case in the present study, single-photon ionization can occur during the start and end of the laser pulse. The contributions from the turn-on and the turn-off of the pulse should be independent of pulse length, and should thus give rise to a constant background ionization probability. The contributions could interfere with each other, but the frequency of this interference should depend only on the characteristics of the turn-on and turn-off. The frequency of the observed oscillations in figure 1 is not ascribed to this frequency difference, as explained below.

The second reason for the dominance of single-photon ionization is provided by the large oscillations in the ionization probability shown in figure 1. The magnitude of these oscillations is the same for all three scaled curves, which suggests that this feature is also due to single-photon processes. Previous photoionization experiments (Covington *et al* 2002) point towards an explanation: just above the  $\text{Ne}^{2+} \ ^3\text{P}^e$  threshold,  $\text{Ne}^+$  has autoionizing Rydberg series converging to the  $^1\text{D}^e$  and  $^1\text{S}^e$  thresholds of  $\text{Ne}^{2+}$  with the  $n = 6$  states attached to the  $^1\text{D}^e$  threshold and the  $n = 4$  states attached to the  $^1\text{S}^e$  threshold lying about 1 eV above the  $^3\text{P}^e$  threshold.

Analysis of the final-state wavefunction confirms that, at the shortest pulse lengths, population of Rydberg states just above the ionization threshold is the main contribution to the ionization yield. The oscillations appear because during the laser pulse, these Rydberg series converging to the  $^1\text{D}^e$  and  $^1\text{S}^e$  threshold are continuously populated and depopulated. For very long laser pulses, the transient population in these states will be small compared to the population in resonantly populated states. In short pulses, however, the population in these transient states may be significant, and depend strongly on the actual pulse parameters, including the turn-on and turn-off of the pulse. These oscillations appear prominently in the ionization yields since the dominant ionization process for long pulses requires absorption of two photons, whereas excitation of these autoionizing states only requires absorption of a single photon. Both effects combined mean that for short pulses single-photon ionization processes may be quite significant even though the central photon energy is well below the single-photon ionization threshold.

Figure 2 compares the ionization probability obtained for an intensity of  $10^{14} \text{ W cm}^{-2}$  with a straight-line fit. For this fit, only pulse lengths with 6 or more cycles at peak intensity are included. At the shortest pulse lengths, uncertainties in the photon energy may enhance the ionization probability and these enhancements should not be included in the fit. The slope of the straight-line fit to the ionization probability should correspond to the two-photon ionization rate of  $\text{Ne}^+$  at a photon energy of 38.4 eV. From this slope, we obtain an ionization rate of  $8.7 \pm 0.4 \times 10^{11} \text{ s}^{-1}$ . This two-photon ionization rate is consistent with the ionization rates obtained in the previous R-matrix-Floquet calculations (Hamonou and van der Hart 2008). Unfortunately, a precise comparison with the R-matrix-Floquet rates can not be made. The photon energy is very close to the threshold for leaving  $\text{Ne}^{2+}$  in the  $2s2p^5 \ ^1\text{P}^o$  state, and the R-matrix-Floquet approach encounters difficulties close to such thresholds. The Floquet R-matrix needs to be propagated to very large distances, making the calculations unfeasible. In addition, the photon energy in the present calculations is not as

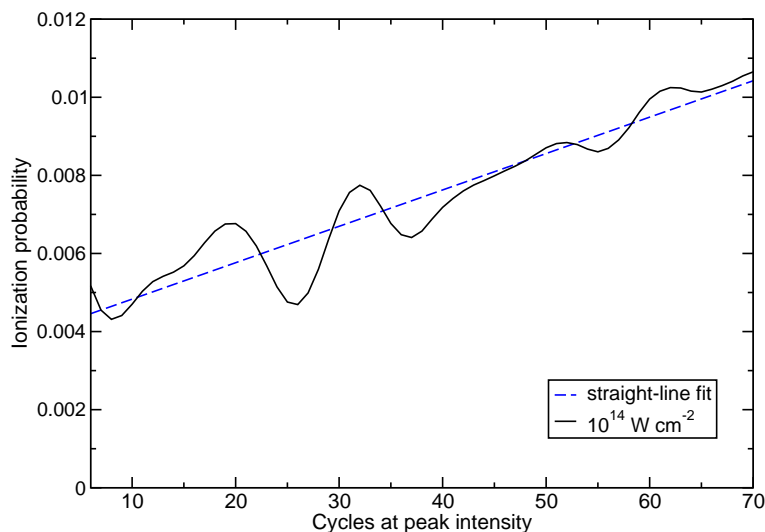


**Figure 2.** (Colour online) Ionisation probability of  $\text{Ne}^+$  irradiated by laser light with a photon energy of 38.4 eV and a peak intensity of  $10^{14} \text{ W cm}^{-2}$  (black solid line), compared with a straight-line fit to the ionization probabilities (blue dashed line). The slope of the straight-line fit approximates the two-photon ionization rate of  $\text{Ne}^+$ .

well-defined as in the R-matrix-Floquet calculations due to the finite pulse length. Nevertheless, a comparison with ionization rates at slightly smaller photon energies shows that the two different approaches are consistent with each other.

Figure 3 compares the ionization probabilities obtained for an intensity of  $10^{13} \text{ W cm}^{-2}$  and  $2 \times 10^{13} \text{ W cm}^{-2}$  with straight-line fits. The figure demonstrates clearly that the uncertainty in the slope of the straight-line fit increases significantly with decreasing intensity due to the increase in the relative magnitude of the oscillations. For an intensity of  $2 \times 10^{13} \text{ W cm}^{-2}$ , we find an ionization rate of  $7.7 \pm 1.0 \times 10^{10} \text{ s}^{-1}$ , and for an intensity of  $10^{13} \text{ W cm}^{-2}$ , we find an ionization rate of  $2.8 \pm 0.6 \times 10^{10} \text{ s}^{-1}$ . These ionization rates show a significant deviation from the expected  $I^2$  scaling. The ratio between the ionization rate at  $10^{14} \text{ W cm}^{-2}$  and  $2 \times 10^{13} \text{ W cm}^{-2}$  is 11.3 as opposed to a ratio of 25 expected from  $I^2$  scaling. This may point towards a significant influence of resonances on the ionization process. When resonant states couple strongly, the assumptions from non-degenerate perturbation theory are no longer valid and one should use degenerate perturbation theory. We should note that a similar deviation from the  $I^2$  scaling has also been seen in R-matrix-Floquet calculations at a photon energy of 38.25 eV in which the intensity was varied between  $10^{12} \text{ W cm}^{-2}$  and  $10^{14} \text{ W cm}^{-2}$ .

To estimate whether autoionizing states may affect experimental ionization yields, we need to consider experimental pulses in more detail. Typical FEL pulses have a duration of up to about 25 fs, whereas the present calculations extend to pulses with a length of 70 cycles, corresponding to about 7.5 fs. Thus experimental pulses can be about a factor 3 longer than the longest pulses considered here. At an intensity of  $10^{14} \text{ W cm}^{-2}$ , from the present calculations one would thus expect the two-photon ionization contribution to be about a factor 5 larger than the single-photon ionization contribution. Figure 2 shows that the magnitude of the oscillations is decreasing with

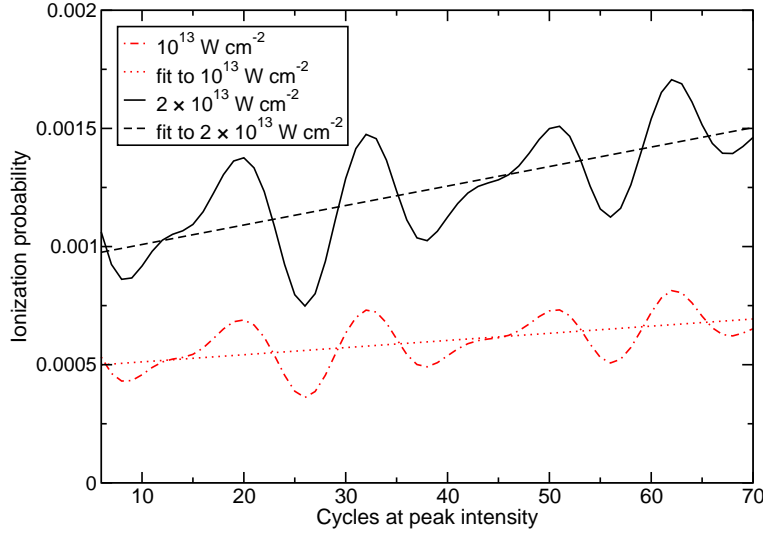


**Figure 3.** (Colour online) Ionisation probability of  $\text{Ne}^+$  irradiated by laser light with a photon energy of 38.4 eV and a peak intensity of  $2 \times 10^{13} \text{ W cm}^{-2}$  (black solid line) and  $10^{13} \text{ W cm}^{-2}$  (red dot-dashed line), compared with straight-line fits to the ionization probabilities for  $2 \times 10^{13} \text{ W cm}^{-2}$  (black dashed line) and  $10^{13} \text{ W cm}^{-2}$  (red dotted line). The slope of the straight-line fit approximates the two-photon ionization rate of  $\text{Ne}^+$ .

increasing pulse length. We hence estimate that the magnitude of the oscillations would be on the order of 2% of the total ionization yield, with an average of about 1%. The effects would, however, be substantially more important for lower intensities, with magnitudes of the oscillations in the order to 10-15% of the total ionization yield. This is due to the relatively smaller contribution from the two-photon ionization process and due to the slower decrease of the magnitude of the oscillations.

The turn-on and turn-off used in the present calculations influence the population of the autoionizing states. For the current pulse shape, the turn-on and turn-off will primarily enhance population in autoionizing states very close to the  $^1\text{D}^e$  threshold, which contribute less to the ionization yield than the autoionizing states just above the  $^3\text{P}^e$  threshold. However, when the turn-on and turn-off are elongated to a six-cycle turn-on and turn-off, we find a significant increase in the ionization yield, since the frequency components of the turn-on and turn-off are now nearly resonant with the autoionizing states just above the  $^3\text{P}^e$  threshold. The actual shape of the laser field can thus play a major role in the  $\text{Ne}^+$  ionization mechanism at photon energies just below the ionization threshold.

Finally, it is important to note that even though a good amount of atomic structure is included, the amount included is rather limited. This is in particular true for the states of the residual  $\text{Ne}^{2+}$  ion. In addition, the calculations are carried out within a finite box. The imposition of boundary conditions at the box radius will affect high-lying Rydberg states. As a consequence, the  $\text{Ne}^+$  states will not necessarily be in their exact position. The appearance of the oscillations depends critically on the position of the autoionizing resonances. As a consequence, the oscillations in the ionization probabilities for the real  $\text{Ne}^+$  ion may differ significantly from the ones presented in 1. However, the overall behaviour of the ionization probabilities, a



large value for short pulses, followed by a rapid initial decrease and a slow increase superimposed by oscillations, should remain. The general physical principles of the competition between single-photon ionization and two-photon ionization do not depend on the exact location of the autoionizing states.

The direct experimental observation of the oscillations in the ionization yields would require carefully controlled laser pulses. The shape of the turn-on and turn-off, as well as the exact photon energy, may influence the outcomes substantially. FEL XUV pulses can currently not be controlled sufficiently to observe such oscillations, as shape and photon energy may vary substantially from pulse to pulse. For these pulses, one would expect to obtain a statistical average, and the present calculations thus suggest that obtained ionization yields at 38.4 eV may have a contribution due to single-photon excitation of autoionizing resonances.

In conclusion, we have obtained ionization probabilities for  $\text{Ne}^+$  irradiated by a laser pulse with a photon energy of 38.4 eV and intensities between  $10^{13} \text{ W cm}^{-2}$  and  $10^{14} \text{ W cm}^{-2}$  as a function of pulse length. Three main features are identified in the ionization yields: For very short pulses, a large ionization probability is obtained due to the energy broadening of the pulse. For longer pulses, an increase in the ionization probability is obtained due to two-photon ionization with a rate consistent with the rates obtained in previous work. The ionization probabilities show large oscillations with pulse length due to the off-resonant transfer of population between the ground state and autoionizing states between the  $^3\text{P}^e$  and  $^1\text{S}^e$  thresholds of  $\text{Ne}^{2+}$ . As a consequence we find that, for the present pulse shape, a pulse length of 5 fs is required at an intensity of  $10^{14} \text{ W cm}^{-2}$  for the contribution to the ionization probability from two-photon ionization to match the contribution from single-photon ionization. For an intensity of  $2 \times 10^{13} \text{ W cm}^{-2}$ , a pulse length of about 15 fs is required.

Key to the interpretation of the present ionization probabilities is the presence of autoionizing states just above the ionization threshold. Such states are not present in single ionization of noble-gas atoms, which have been the main focus of experiment and theory. As a consequence, the influence of such states on the ionization mechanism has not received significant attention. The present results suggests, however, that these states may influence ionization processes significantly. Hence, there is a need for the continued development of theoretical methods capable of investigating strong-field processes in complex atoms.

## Acknowledgments

LH acknowledges funding by the European Social Fund as part of the Building Sustainable Prosperity programme. ML and HvdH acknowledge funding by the UK Engineering and Physical Sciences Research Council under grant ref. nos. EP/E000223/01 and EP/E016588/01.

## References

- Burke P G, Francken P and Joachain C J 1991 *J. Phys. B: At. Mol. Opt. Phys.* **24**, 761
- Clementi E and Roetti C 1974 *At. Data. Nucl. Data Tables* **14** 177-478
- Colgan J and Pindzola M S 2002 *Phys. Rev. Lett.* **88** 173002
- Covington A V, Aguilar A, Covington I R, Gharaibeh M F, Hinojosa G, Shirley C A, Phaneuf R A, Alvarez I, Cisneros C, Dominguez-Lopez I, Sant'Anna M M, Schlachter A S, McLaughlin B M and Dalgarno A, 2002 *Phys. Rev A* **66** 062710

- Feist J, Nagele S, Pazourek R, Persson E, Schneider B I, Collins L A, and Burgdörfer J 2008 *Phys. Rev. A* **77** 043420
- Feng L and van der Hart H W 2003 *J. Phys. B: At. Mol. Opt. Phys.* **36** L1-L7
- Fritzsche S, Grum-Grzhimailo A N, Gryzlova E V and Kabachnik N M 2008 *J. Phys. B: At. Mol. Opt. Phys.* **41** 165601
- Guan XX, Noble C J, Zatsarinny O, Bartschat K and Schneider B I 2008 *Phys. Rev. A* **78** 053402
- Guan XX, Zatsarinny O, Noble C J, Bartschat K and Schneider B I 2009 *J. Phys. B: At. Mol. Opt. Phys.* **42** 134015
- Hamonou L, van der Hart H W, Dunseath K M and Terao-Dunseath M 2008 *J. Phys. B: At. Mol. Opt. Phys.* **41** 015603
- Hamonou L and van der Hart H W 2008 *J. Phys. B: At. Mol. Opt. Phys.* **41** 121001
- Kurka M, Rudenko A, Foucar L, Kühnel K U, Jiang Y H, Ergler Th, Havermeier T, Smolarski M, Schössler S, Cole K, Schöffler M, Dörner R, Gensch M, Düsterer S, Treusch R, Fritzsche S, Grum-Grzhimailo A N, Gryzlova E V, Kabachnik N M, Schröter C D, Moshhammer R and Ullrich J 2009 *J. Phys. B: At. Mol. Opt. Phys.* **42** 141002 **33** 597
- Laulan S and Bachau H 2003 *Phys. Rev. A* **68** 013409
- Lysaght M A, Burke P G and van der Hart H W 2008 *Phys. Rev. Lett.* **101** 253001
- Lysaght M A, Burke P G and van der Hart H W 2009a *Phys. Rev. Lett.* **102** 193001
- Lysaght M A, van der Hart H W and Burke P G 2009b *Phys. Rev. A* **79** 053411
- McLaughlin B M and Bell K L 2000 *J. Phys. B: At. Mol. Opt. Phys.* **33** 597
- Moshhammer R *et al* 2007 *Phys. Rev. Lett.* **98** 203001
- Parker J S, Doherty B J S, Taylor K T, Schultz K D, Blaga C I and DiMauro L F 2006 *Phys. Rev. Lett.* **96** 133001
- Rudenko A *et al* 2008 *Phys. Rev. Lett.* **101** 073003
- Sorokin A A, Wellhöfer M, Bobashev V, Tiedtke K and Richter M 2007 *Phys. Rev. A* **75** 051402(R)
- van der Hart H W 2005 *Phys. Rev. Lett.* **95** 153001
- 2006 *Phys. Rev. A* **73** 023417